Synchrotron radiation intensity and energy of runaway electrons in EAST Tokamak

Y. K. Zhang(张永宽),[1,2] R. J. Zhou(周瑞杰),[1,*] L. Q. Hu(胡立群),[1] M. W. Chen(陈美文),[1,2] Y. Chao(晁燕)[1,2] and EAST team.

1) *Institute of Plasma Physics, Hefei institutes of Physical Science, Chinese Academy of Sciences, Hefei 230031, China*

2) *University of Science and Technology of China, Hefei 230026, China*

*Corresponding author. E-mail: rjzhou@ipp.ac.cn

Abstract

A detailed analysis of the synchrotron radiation intensity and energy of runaway electrons are presented for EAST. In order to make the energy of the calculated runaway electrons more accurate, we take the shafranov shift into account. The results of the analysis show that the synchrotron radiation intensity and energy of runaway electrons did not reach the maximum at the same time. The energy of runaway electrons reached the maximum value first, and then the synchrotron radiation intensity of the runaway electrons reached the maximum. We also analyzed the runaway electrons density, and it shows the density of runaway electrons continuously increased. For this reason, although the energy of the runaway electrons drops but the synchrotron radiation intensity of the runaway electrons will continue rising for a while.

Key words: Tokamak; runaway electron; synchrotron radiation

PACS Codes: 52.70.Nc, 52.25.Os, 52.35.Hr

1 Introduction

In tokamaks electrons mainly experience two forces, one is the electric field force F_e that can make the electrons accelerate, the other is the force of collisions with the plasma particles that can decelerate the electrons.

$$F_d = -\frac{n_e e^4 ln\Lambda}{4\pi\varepsilon_0^2 m_e v^2}\left(1+\frac{Z_{eff}+1}{\gamma}\right) \tag{1}$$

where γ is the relativistic factor [1]. As the energy of electrons increases, the collision frequency drops rapidly [2], resulting in a rapid decrease in F_d. When $Fd < Fe$, electrons can be accelerated by the electric field to several tens of MeV or even higher energy in EAST [3].

With the increasing volume of tokamak devices, the energy of runaway electrons is getting higher and higher. In future tokamaks such as ITER, the energy of runaway electrons can even reach 100 MeV [4]. Such high energy electrons can be a serious threat to the tokamak [5]. To study the energy and intensity evolution of those high-energy runaway electrons in

experiments, it is extremely important to diagnose the electron parameters effectively and correctly.

In general, the generation of runaway electrons can be divided into two categories: one is in the current ramp-up phase, and the other is during the fast plasma terminations due to plasma disruptions or the killer pellet injection [6]. The runaway electrons generated in fast plasma terminations have a short duration and change rapidly. The frame frequency of the infrared cameras existing on the EAST is low. It is difficult to study the change of runaway electrons. However the infrared camera can be used to study the evolution of runaway electrons in the current ramp-up phase.

The typical methods is measuring the thick-target bremsstrahlung emission or photo-neutrons resulting by runaway electrons when they are lost and then impact the limiter or vessel structures. Detection of the synchrotron radiation emitted by runaway electrons by

infrared cameras is the best way to diagnose high-energy runaway electrons which were constrained in the core of the plasma directly [7]. In the current ramp-up phase, the vast majority of high-energy runaway electrons are constrained in the core of the plasma, only a small part of the runaway electrons lost and impact the limiter or vessel structure. In simple terms, detecting the runaway electrons by an infrared camera can reflect the situation of the runaway electrons existing in the plasma better.

In this paper, we carry out detailed analysis of the synchrotron radiation intensity and energy of runaway electrons in EAST. In section 2, we present the calculation and evolution of the pitch angle of the runaway electrons. In section 3, we calculated the energy of the runaway electrons. In section 4, we analyzed the evolution of the runaway electron synchrotron radiation and the evolution of the density of runaway electrons. The conclusions are summarized in section 5.

2 The pitch angle of the runaway electrons

It is generally defined $\tan\theta_P = v_\perp / |v_\parallel|$, where $v_\perp$ and $v_\parallel$ are the transverse and longitudinal velocities of the runaway electrons respect to the confining magnetic field, respectively, θ_p is the pitch angle. In general, θ_p ＜0.2 is a small amount , it can be considered $\theta_p \approx \tan\theta_p = v_\perp / |v_\parallel|$.
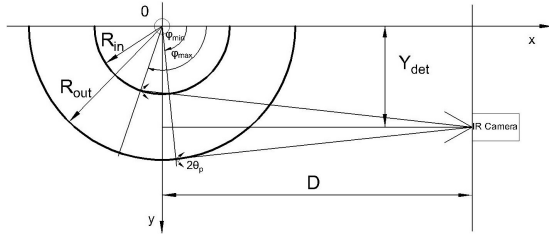

FIG. 1. Relative position of the beam of runaway electrons and the infrared camera in the plane z=0. R_{in} and R_{out} are the inner and outer major radius of the beam.

Schematic of the relative positions of the beam of runaway electrons and the infrared

camera is shown in figure 1. The camera is close to the plasma and viewing tangentially into the plasma from the equatorial plane. The pitch angle of the runaway electrons is θ_p and the synchrotron radiation is emitted in the range of the apex angle of $2\theta_p$.

The analytical treatment of the calculation of the synchrotron radiation spot shape from runaway electrons has been carried out in Ref. 8. The coordinates we used in the calculation are shown in figure 2. The transverse cross sections of the magnetic surfaces and runaway electrons drift orbit are assumed to be nearly circular.

All the subsequent analyses of runaway electrons appeared in current ramp-up phase are based on the discharge shown in Figure 3.
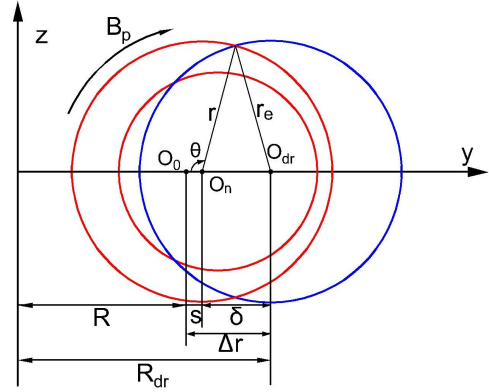

FIG. 2. System of coordinates used in the calculations. The red circle and the blue circle represent the magnetic surface and drift orbit surface of the runaway electrons, respectively. R is the major radius of EAST. s and δ are the Shafranov shift and the distance of runaway electrons drift orbit from the magnetic surfaces, respectively. O_0 is the geometric center of a vacuum vessel.

Under the above infrared camera and runaway electron beam position conditions, the synchrotron radiation emitted along the runaway electron velocity vector falls into the infrared camera whose conditions satisfy the following equation [8]:

$$\pm r\sin\theta \approx [\frac{r\cos\theta}{q(r)R} + \frac{v_\perp\sin(\theta\pm\alpha)}{v_\parallel} + \frac{v_d + v_v}{v_\parallel}]$$

2

$$\times[D+(R\text{-}r\cos\theta)\sin\triangle] \qquad (2)$$

in which $\triangle << 1$ is the range of toroidal angles of the synchrotron radiation can be recorded by the infrared camera($\varphi=\pi/2+\triangle$). r presents the distance between O_0 and the runaway electrons, the value of r varies at different points, and the average is taken here . $v_\perp$ and $v_\parallel$ are the transverse and longitudinal velocities of the runaway electrons respect to the confining magnetic field, respectively. $v_d + v_v/v_\parallel$ is usually small, we will omit it; $\triangle << 1$, so we can omit $(R\text{-}r\cos\theta)\sin\triangle$. We assume $v_\perp/|v_\parallel|\approx\theta_p$. Then the above formula can be written as :

$$\pm r\sin\theta\approx(\frac{r\cos\theta}{q(r)R} \pm \theta_p\sin\theta) \times D \qquad (3)$$

and then

$$\tan(\beta_{inc})=-\tan\theta\approx-\frac{D\times r}{q(r)R(\mp D\theta_p\pm r)} \qquad (4)$$

In the above equations, the upper and lower signs correspond to the case when the magnetic field is directed away from ($v_\parallel< 0$) and toward ($v_\parallel> 0$) the detector, respectively. β_{inc} is the angle between the horizontal line and the long axis of the asymmetrical synchrotron radiation spot.
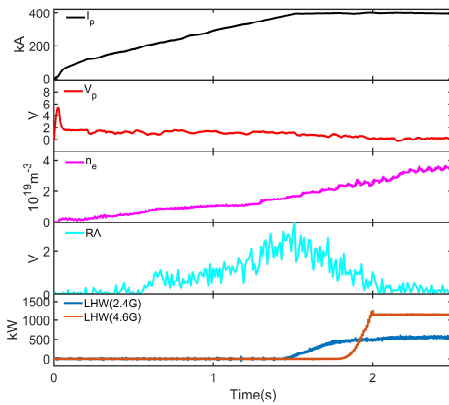
FIG. 3. Time slice of a runaway discharge in the EAST tokamak. The waveforms are plasma current, loop voltage, line-averaged density, RA, power of 2.4G and 4.6G lower hybrid wave.

As shown in figure 4, the β_{inc} angle can be measured from the synchrotron radiation spot of runaway electrons. In the equation (3), only θ_p is unknown, so we can calculate the value of θ_p. The important parameter θ_p for runaway electrons can be obtained from β_{inc}, so β_{inc} is very important. The θ_p calculated by the above method is the average value of the pitch angle. The evolution of the θ_p is shown in figure 5.
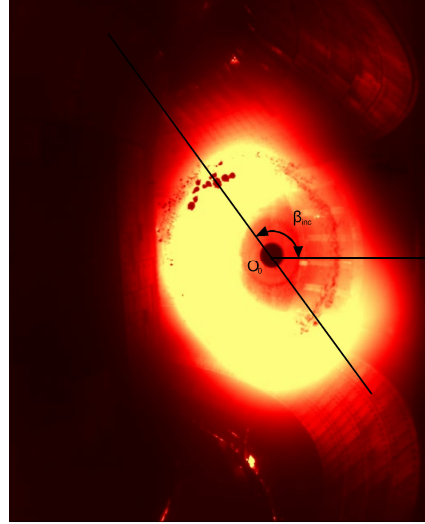
FIG. 4. Synchrotron radiation spot from the runaway electron beam recorded by the infrared camera in EAST.
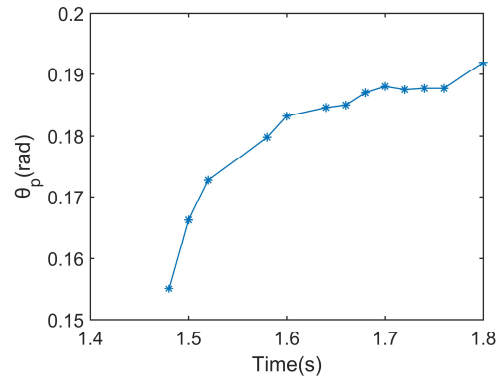
FIG. 5. The pitch angles of runaway electrons

3 The energy of the runaway electrons

The energy of the runaway electron beam can be gained from its drift orbit shift. The drift orbit shifted from the magnetic surface by a distance δ, to first-order approximation [9], by

$$\delta = q\gamma m_e c/eB_0 \qquad (5)$$

3

Where q is the safety factor, the runaway electrons exist around the $q=2$ rational surface. In the following calculations, the q value is taken to be $q=2$ [10]. δ is the distance of runaway electrons drift orbit from the magnetic surfaces, $\delta = \Delta r - s$. As shown in figure 6(marked in blue), the Δr can be measured from the pictures of synchrotron radiation spot of the runaway electron beam. Shafranov shift $0.7\text{cm} < s < 1.4\text{cm}$, here we take $s = 1\text{cm}$. Compared with the Δr in the middle (marked in blue) of the runaway electron beam, most of the Δr at the edge (marked in black) have less than 10% errors (before 1.62s). The maximum errors (before 1.62s) of Δr and $\Delta r - s$ are less than 15% and 16%, respectively. The toroidal magnetic field $B_0 = 1.8\text{T}$. So the average energy of the runaway electrons can be calculated by the following formula:

$$E = \frac{(\Delta r - s)ecB_0}{q} \quad (6)$$

As shown in figure 8, the energy of the runaway electrons rose before 1.48s and then

decreased. The decrease of runaway electron energy is due to the increase of plasma density, which leads to the increase of drag and the decrease of loop voltage, resulting in the decrease of power.
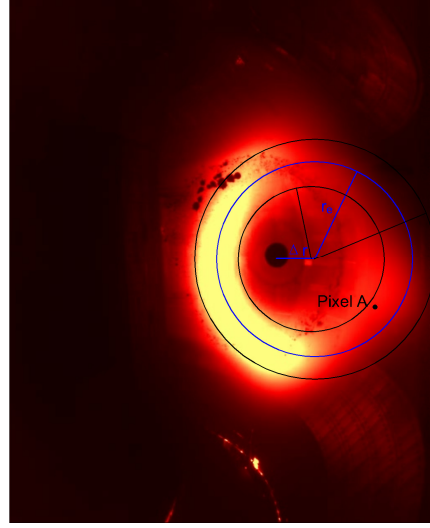

FIG. 6. Synchrotron radiation spot from the runaway electrons beam in EAST. Δr represents the shift of the center of the runaway electrons orbit. r_e is the radius of the runaway electrons orbit.
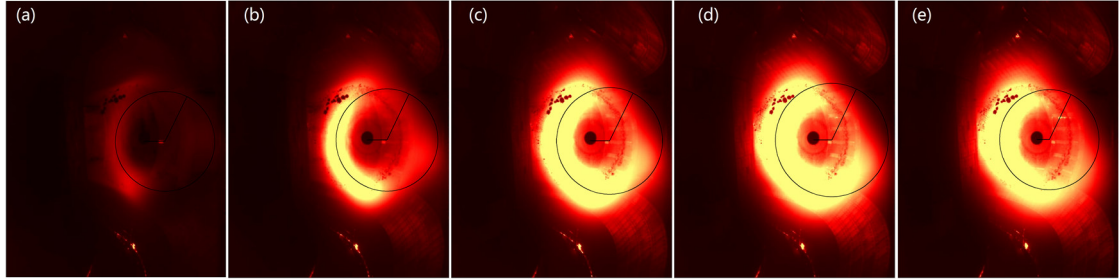

FIG. 7   The evolution of the synchrotron radiation spot emitted by the runaway electrons. The corresponding moments of (a),(b),(c),(d) ,(e) are 1.46s, 1.52s, 1.58s, 1.64s and 1.70s.
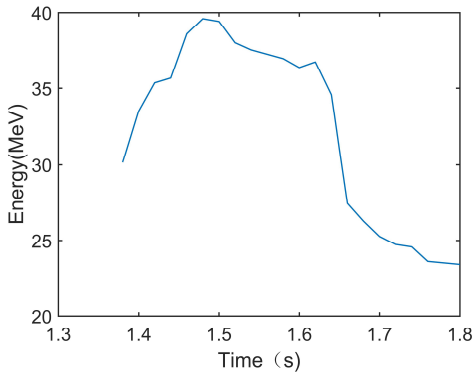
The energy rose before 1.48s and then decreased.

4 Synchrotron radiation intensity of runaway electrons

The synchrotron radiation intensity of runaway electrons recorded by the infrared camera at pixel A is shown in figure 9. The overall trend of synchrotron radiation intensity of runaway electrons recorded by the infrared camera was enhanced first and then weakened.

In figure 9, the synchrotron radiation intensity recorded by the infrared camera and

FIG. 8. The energy of the runaway electrons.

the energy of runaway electrons did not reach their maximum at the same time. The synchrotron radiation intensity recorded by the infrared camera is related to energy, density and θ_p of runaway electrons in EAST. Taking energy and θ_p into account, the change of radiation spectra of a single electron between 1.5s and 1.6s is small. Furthermore, taking a certain error into account at 1.6s, the change of the spectrum (from 2.5μm to 5μm) is still small. But the synchrotron radiation intensity observed by the infrared camera varied greatly. So the density of runaway electron certainly increased.
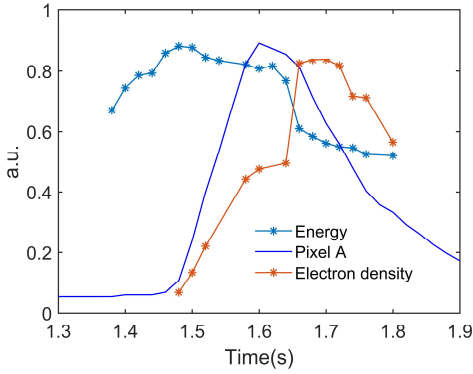

FIG. 9. Relationship between synchrotron radiation intensity, energy and density of runaway electrons. They did not reach their maximum at the same time.
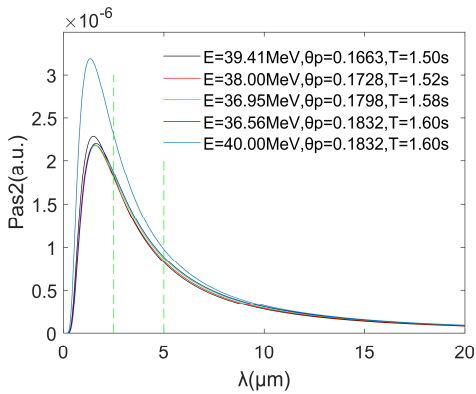

FIG. 10. The synchrotron radiation spectra of single runaway electron in EAST with R=1.86m, B_T=1.8T. The two vertical dashed lines are 2.5μm and 5μm, respectively.

The density of runaway electrons can be calculated by the synchrotron radiation intensity recorded by the infrared camera and the synchrotron radiation spectra of single runaway electron in EAST. The infrared cameras can observe infrared rays in the wavelength range of 2.5μm to 5μm. We integrated the spectra from 2.5μm to 5μm to obtain the radiation intensity of a single electron can be detected. And then the intensity of the synchrotron radiation measured by the infrared camera divided by the radiation intensity of a single electron, so as to get the relative density of runaway electrons. As shown in figure 9, it is clearly that the density of runaway electrons increased before 1.7s. As shown in figure 3, the increase of runaway electrons density occurs in the density ramp-up phase. It is possible that the increase of plasma density leads to the increase of runaway electrons density, but no strong evidence has been found. During 1.5s-1.6s, the increase of runaway electrons density led to the synchrotron radiation intensity recorded by the infrared camera increasing though the energy of runaway electrons decreased.

5   Summary

Synchrotron radiation is a powerful tool for diagnosing high-energy runaway electrons that are confined in the core of the plasma. In this paper, we have presented a detailed analysis of the energy, synchrotron radiation intensity and density of runaway electrons.

The energy of the runaway electron beam can be gained from its drift orbit shift. The energy of the runaway electrons rose before 1.48s and then decreased. The decrease of runaway electron energy is due to the increase of plasma density, which leads to the increase of drag and the decrease of loop voltage, resulting in the decrease of power.

The synchrotron radiation intensity of runaway electrons recorded by the infrared camera and the energy of runaway electrons did not reach their maximum at the same time. The

5

main reason why they did not reach the maximum at the same time was that the density of runaway electrons was rising when the energy of runaway electrons began to decrease. The increase of runaway electrons density led to the synchrotron radiation intensity recorded by the infrared camera increasing though the energy of runaway electrons decreased.

Acknowledgments

References

[1] Fussmann G 1979 *Nuclear Fusion*. **19** 327

[2] Dreicer H 1959 *Physical Review*. **115** 238

[3] Zhou R J , Hu L Q, Li E Z, et al. 2013 *Plasma Physics and Controlled Fusion*. **55** 055006

[4] Bakhtiari M , Kramer G J, Takechi M, et al. 2005 *Physical review letters*. **94** 215003

[5] Yoshino R , Kondoh T, Neyatani Y, et al. 1997 *Plasma physics and controlled fusion*. **39** 313

[6] Esposito B , Martın-Solıs J R, Poli F M, et al. 2003 *Physics of Plasmas*. **10** 2350-2360

[7] Jaspers R , Lopes Cardozo N J, Donne A J H, et al. 2001 *Review of Scientific Instruments*. **72** 466-470

[8] Pankratov I M 1996 *Plasma Physics Reports*. **22** 535

[9] Guan X , Qin H, Fisch N J 2010 *Physics of Plasmas*. **17** 092502

[10] Zhou R J , Pankratov I M, Hu L Q, et al. 2014 *Physics of Plasmas*. **21** 063302